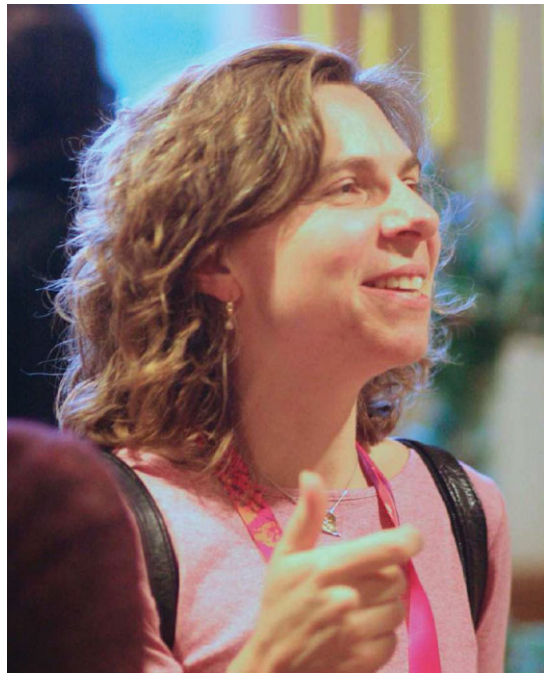


## **Session IV**

### **Sources and sinks of light elements**



Suzanne Talon



Takuji Tsujimoto

# Light elements as diagnostics on the structure and evolution of low-mass stars

Suzanne Talon<sup>1</sup> and Corinne Charbonnel<sup>2,3</sup>

<sup>1</sup>RQCHP, Département de physique, Université de Montréal, C.P. 6128, succ. centre-ville,  
Montréal, Québec, H3C 3J7  
email: suzanne.talon@umontreal.ca

<sup>2</sup>Geneva Observatory, University of Geneva, ch. des Maillettes 51, 1290 Versoix, Switzerland  
email: Corinne.Charbonnel@unige.ch

<sup>3</sup>Laboratoire d’Astrophysique de Toulouse-Tarbes, Université de Toulouse, CNRS UMR 5572,  
14 Av. E. Belin, 31400 Toulouse, France

**Abstract.** Low-mass stars exhibit, at all stages of their evolution, the signatures of complex physical processes that require challenging modelling beyond standard stellar theory. In this review, we focus on lithium depletion in low-mass stars. After dissecting the Li dip, we discuss how large scale mixing due to rotation and internal gravity waves may interact to explain this feature. We also briefly discuss the impact that is expected on Population II stars.

**Keywords.** Hydrodynamics – instabilities – turbulence – waves – stars: abundances, evolution, interiors, rotation

---

## 1. The lithium dip, atomic diffusion and rotation-induced mixing

During the last couple of decades, it became obvious that the art of modeling stars in the 21<sup>st</sup> century strongly relies on the art of modelling transport processes. Observational evidences now give precise clues on the various processes that transport angular momentum and chemical elements in the radiative regions of low-mass stars, at various stages of their evolution. One of the most striking signatures of transport processes in low-mass stars is the so-called Li dip (see Fig. 1). This drop-off in the Li content of main-sequence F-stars in a range of  $\sim 300$  K centered around 6700 K was discovered in the Hyades by Wallerstein *et al.* (1965); its existence was later confirmed by Boesgaard & Tripicco (1986). This feature appears in all open clusters older than  $\sim 200$  Myr, as well as in field stars (Balachandran 1995), an indication that it is a phenomenon occurring on the main sequence.

Michaud’s (1986) original suggestion that this structure is shaped by gravitational settling (causing the drop in Li abundance on the cool side of the dip as the surface convection zone shrinks) and radiative levitation (which explains the rise on the warm side of the dip) suffers from two serious drawbacks:

- The expected concomitant underabundances of heavier elements (C, N, O, Mg, Si) are not observed in cluster stars (Takeda *et al.* 1998; Varenne & Monier 1999; Gebran *et al.* 2008).
- In this framework, Li is not destroyed; it settles and accumulates in a buffer zone below the convective envelope. Li should thus be dredged-up as a star enters the Hertzsprung gap and this is not observed, neither in the field nor in open cluster stars (Pilachowski *et al.* 1988; Deliyannis *et al.* 1997).

Boesgaard (1987) noticed that the effective temperature of the dip is also associated with a sharp drop in rotation velocities (see Fig. 1). Rotation was then suggested to play a

dominant role in this mass range. To properly model rotation-induced mixing, one must follow the time evolution of the angular momentum distribution within a star, taking into account *all* relevant physical processes: contraction/expansion caused by stellar evolution, mass loss or accretion, tidal effects, as well as internal redistribution of angular momentum through meridional circulation, turbulence, magnetic torques and waves.

### 1.1. Shaping the warm side of the dip with wind driven circulation

The description of the internal physical processes related to stellar rotation greatly improved during the last two decades. Here, we review the results of the application of Zahn's (1992) model of rotation-induced mixing, using the same free parameters as those required to explain abundance anomalies in more massive stars (see Maeder & Meynet 2000). In this framework, transport of angular momentum is dominated by the Eddington-Sweet meridional circulation and shear instabilities.

In the dip region, the evolution of a star's angular momentum is influenced by various mechanisms depending on its effective temperature.

- Stars with  $T_{\text{eff}}$  higher than  $\sim 6900$  K have a shallow convective envelope and are not spun down by a magnetic torque. These stars soon reach a stationary regime where there is no net flux of angular momentum<sup>†</sup>, in which meridional circulation and shear-induced turbulence counterbalance each other. The associated weak mixing is just sufficient to counteract atomic diffusion. These rotating models account nicely for the observed constancy of Li and CNO in these stars, and they also explain the Li and Be behaviour in subgiant stars (Palacios *et al.* 2003; Pasquini *et al.* 2004; Smiljanic *et al.* 2009; see also Charbonnel & Lagarde, this Volume). Talon, Richard, & Michaud (2006) showed that the transport coefficients related to rotation-induced mixing lead to normal A stars for rotation velocities above  $\sim 100 \text{ km s}^{-1}$ , and permit Am anomalies below with a mild correlation with rotation, provided a reduction of turbulent mixing by horizontal turbulence is taken into account. Fossati *et al.* (2008) have confirmed observationally this correlation with rotation.

- Between  $\sim 6900$  and  $6600$  K, the convective envelope deepens and a weak magnetic torque, associated with the apparition of a surface dynamo, spins down the outer layers of the star. This creates internal shears and the transport of angular momentum by meridional circulation and shear turbulence increases, leading to a larger destruction of Li and Be, in agreement with the data. The rotating model thus perfectly fits the blue side of the Li and Be dips (Talon & Charbonnel 1998, Charbonnel & Talon 1999, Palacios *et al.* 2003, Pasquini *et al.* 2004; Smiljanic *et al.* 2009).

- Stars on the cool side of the Li dip ( $T_{\text{eff}} < 6600$  K) have an even deeper convective envelope sustaining a very efficient dynamo, which produces a strong magnetic torque that spins down the outer layers very efficiently. If we assume that all the angular momentum transport is assured by the wind-driven circulation in these stars<sup>‡</sup>, we obtain too much Li depletion compared to the observations (see Fig. 2). *On the basis of these results, Talon & Charbonnel (1998) suggested that the Li dip corresponds to a transition region where the efficiency of another process for angular momentum transport rises.*

This signature of the existence of new physics can be drawn from studies performed by two other groups. In Théado & Vauclair (2003), where rotation-induced mixing is assumed to be linked to meridional circulation in a solid-body rotating star, the two free parameters associated with this mixing have to be varied by factors of 2 and 260 to fit

<sup>†</sup> In fact, there remains a small flux of angular momentum, just sufficient to counteract the effect of stellar contraction/expansion.

<sup>‡</sup> Let us mention that in the case of large shears meridional circulation is far more efficient than shear for angular momentum transport.

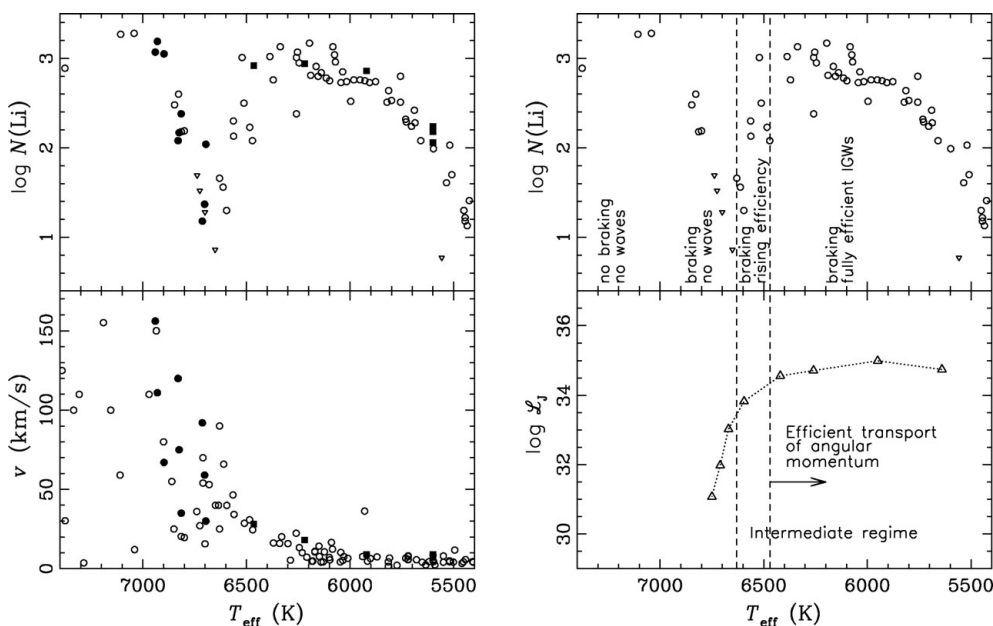


**Figure 1.** (Left) (top) Lithium abundance in the Hyades versus effective temperature (open symbols, data from Burkhardt & Coupy 2000) plus model data (filled symbols). Circles: models where internal gravity waves (hereafter IGWs) are negligible. Squares: models where IGWs are significant (Charbonnel & Talon 2005; Talon & Charbonnel 2005). (bottom) Rotational velocity in the Hyades - unprojected (open symbols, data from Gaigé 1993) plus model data (filled symbols). (Right) (top) Lithium abundance plus approximate dependence of surface braking on effective temperature and the requirements for angular momentum transport for rotational mixing to lead to the formation of the lithium dip (Talon & Charbonnel 1998). (bottom) Filtered angular momentum luminosity of waves below the SLO measuring the efficiency of wave induced angular momentum transport. Adapted from Talon & Charbonnel (2003).

the Li dip. Similarly, Richard *et al.* (priv. comm.) have to change the ad-hoc turbulence they add to reduce atomic diffusion by an order of magnitude along along the Li dip. The strong variation of these *fudge factors* is actually an indication that the *physical processes* at play inside these stars change in that region.

### 1.2. A link with the Sun's rotation

The proposition by Talon & Charbonnel (1998) may be linked to another observation that fails to be reproduced by the pure hydrodynamic models, namely the flat solar rotation profile revealed by helioseismology (Brown *et al.* 1989; Kosovichev *et al.* 1997; Couvidat *et al.* 2003; García *et al.* 2007). At the solar age, models relying only on turbulence and meridional circulation for momentum transport predict large angular velocity gradients that are not present in the Sun (Pinsonneault *et al.* 1989; Chaboyer *et al.* 1995; Talon 1997; Matias & Zahn 1998). This indicates that another process participates to the transport of angular momentum in solar-type stars.

Two candidates have been examined. The first rests on the possible existence of a magnetic field within the radiation zone (Charbonneau & MacGregor 1993; Eggenberger *et al.* 2005). The second invokes traveling internal gravity waves (hereafter IGWs) generated at the base of the convection envelope (Schatzman 1993; Zahn *et al.* 1997; Kumar & Quataert 1997; Talon, Kumar & Zahn 2002). For either of these solutions to be convincing, they must be tested with numerical models coupling these processes with rotational

instabilities and should explain all the aspects of the problem, including the lithium evolution with time.

The Li data suggest that the efficiency of the additional process is linked to the growth of the convective envelope in stars with effective temperatures around  $T_{\text{eff}} \simeq 6600$  K. As we shall see below, this is a characteristic of IGWs.

## 2. IGWs generation and momentum extraction in low-mass stars

In the Earth's atmosphere, wave-induced momentum transport is a key process in the understanding of several phenomena, the best known being the quasi-biennial oscillation of the stratosphere. In astrophysics, IGWs have initially been invoked as a source of mixing for chemicals (Press 1981; García Lopez & Spruit 1991; Schatzman 1993; Montalban 1994; Montalban & Schatzman 1996, 2000; Young *et al.* 2003). Ando (1986) studied the transport of angular momentum associated with standing gravity waves in Be stars. He was the first to clearly state, in the stellar context, that IGWs carry angular momentum from the region where they are excited to the region where they are dissipated. Traveling IGWs have since been invoked as an important source of angular momentum redistribution in single stars (Schatzman 1993; Kumar & Quataert 1997; Zahn, Talon & Matias 1997, Talon *et al.* 2002; Charbonnel & Talon 2005).

### 2.1. IGWs generation and wave spectrum

Two different processes contribute to IGWs excitation at the border of convective regions: convective overshooting in an adjacent stable region (García López & Spruit 1991; Kiraga *et al.* 2003; Rogers & Glatzmaier 2005a, 2005b), and Reynolds stresses in the convection zone (Goldreich & Kumar 1990; Balmforth 1992; Goldreich, Murray & Kumar 1994). In our studies, we shall use the second mechanism, which has been calibrated on solar p-modes and, thus, seems more reliable at this time. This gives a lower limit to the correct/total wave flux although neglecting the other excitation mechanism remains the weakest point of wave-induced transport models (see Charbonnel & Talon 2007 for a complete discussion on wave excitation and numerical simulations).

If we assume that prograde and retrograde waves are produced with the same efficiency and if they are damped in the same way as they propagate inside the star, then waves have no net impact on the angular momentum distribution. It is thus important to treat wave damping properly. In Talon *et al.* (2002), we showed that the development of a double-peaked shear layer (SLO, for Shear Layer Oscillation), acts as a filter for waves and that, when the core is rotating faster than the surface, the asymmetry of this filter produces momentum extraction.

In Talon & Charbonnel (2005), we developed a formalism to incorporate the contribution of IGWs to the transport of angular momentum and chemical elements in stellar models on secular time-scales. Using only this filtered flux, it is possible to follow the contribution of internal waves over long (evolutionary) time-scales. We use the formalism developed by Goldreich & Kumar (1990) and Goldreich *et al.* (1994) to estimate the angular momentum luminosity  $\mathcal{L}_J$  below the convective envelope (see also Kumar & Quataert 1997). The local momentum luminosity of waves is then given by

$$\mathcal{L}_J(r) = \sum_{\sigma, \ell, m} \mathcal{L}_{J\ell, m}(r_{\text{cz}}) \exp[-\tau(r, \sigma, \ell)] \quad (2.1)$$

where 'cz' refers to the base of the convection zone.  $\tau$  corresponds to the integration of

the local damping rate, and takes into account the mean molecular weight stratification

$$\tau(r, \sigma, \ell) = [\ell(\ell + 1)]^{\frac{3}{2}} \int_r^{r_c} (K_T + \nu_v) \frac{NN_T^2}{\sigma^4} \left( \frac{N^2}{N^2 - \sigma^2} \right)^{\frac{1}{2}} \frac{dr}{r^3} \quad (2.2)$$

(Zahn *et al.* 1997). In this expression,  $N_T^2$  is the thermal part of the Brunt-Väisälä frequency,  $K_T$  is the thermal diffusivity and  $\nu_v$  the (vertical) turbulent viscosity.  $\sigma$  is the local, Doppler-shifted frequency

$$\sigma(r) = \omega - m [\Omega(r) - \Omega_{cz}] \quad (2.3)$$

and  $\omega$  is the wave frequency in the reference frame of the convection zone. Let us mention that, in this expression for damping, only the radial velocity gradients are taken into account. This is because angular momentum transport is dominated by the low frequency waves ( $\sigma \ll N$ ) for which horizontal gradients are much smaller than vertical ones.

When meridional circulation, turbulence, and waves are all taken into account, the evolution of angular momentum follows

$$\rho \frac{d}{dt} [r^2 \Omega] = \frac{1}{5r^2} \frac{\partial}{\partial r} [\rho r^4 \Omega U] + \frac{1}{r^2} \frac{\partial}{\partial r} \left[ \rho \nu_v r^4 \frac{\partial \Omega}{\partial r} \right] - \frac{3}{8\pi} \frac{1}{r^2} \frac{\partial}{\partial r} \mathcal{L}_J(r), \quad (2.4)$$

(Talon & Zahn 1998) where  $U$  is the radial meridional circulation velocity. This equation takes into account the advective nature of meridional circulation rather than modeling it as a diffusive process and assumes a “shellular” rotation (see Zahn 1992 for details). Horizontal averaging was performed, and meridional circulation is considered only at first order. When we calculate the fast SLO’s dynamics,  $U$  is neglected in this equation. This is justified by the fact that when shears are large such as in the SLO, angular momentum redistribution is dominated by the (turbulent) diffusivity rather than by meridional circulation. However, the complete equation is used when we compute full evolution models as in Charbonnel & Talon (2005).

## 2.2. Shear layer oscillation (SLO) and filtered angular momentum luminosity

One key feature of the wave-mean flow interaction is that the dissipation of IGWs produces an increase in the local differential rotation: this is caused by the increased dissipation of waves that travel in the direction of the shear (see Eqs. 2.2 and 2.3). In conjunction with viscosity, this leads to the formation of an oscillating doubled-peak shear layer that oscillates on a short time-scale (Gough & McIntyre 1998; Ringot 1998; Kumar, Talon & Zahn 1999). This oscillation is similar to the Earth quasi-biennial oscillation that is also caused by the differential damping of internal waves in a shear region.

This SLO occurs if the deposition of angular momentum by IGWs is large enough when compared with (turbulent) viscosity (Kim & MacGregor 2001)†. To calculate the turbulence associated with this oscillation, we rely on a standard prescription for shear turbulence away from regions with mean molecular weight gradients

$$\nu_v = \frac{8}{5} Ri_{crit} K \frac{(rd\Omega/dr)^2}{N_T^2} \quad (2.5)$$

which takes radiative losses into account (Townsend 1958; Maeder 1995). This coefficient is time-averaged over a complete oscillation cycle (for details, see Talon & Charbonnel 2005).

In the presence of differential rotation, the dissipation of prograde and retrograde waves in the SLO is not symmetric, and this leads to a finite amount of angular momentum

† If viscosity is large, a stationary state can be reached.

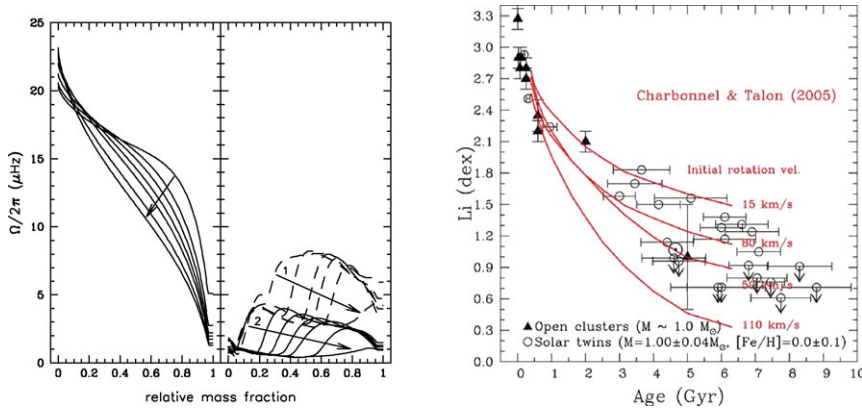


**Figure 2.** (Left) Evolution of the rotation profile in a solar-mass model with and without IGWs. The initial equatorial rotation velocity is  $50 \text{ km s}^{-1}$ , and identical surface magnetic braking is applied. (left) Model without IGWs. Curves correspond to ages of 0.2, 0.5, 0.7, 1.0, 1.5, 3.0 and 4.6 Gy that increase in the direction of the arrow. (right) When IGWs are included, low-degree waves penetrate all the way to the core and deposit their negative angular momentum in the whole radiative region. Curves labelled 1 correspond to ages of 0.2, 0.21, 0.22, 0.23, 0.25 and 0.27 Gy and those labelled 2 to 0.5, 0.7, 1.0, 1.5, 3.0 and 4.6 Gy. From Charbonnel & Talon (2005). (Right) Evolution of surface lithium abundance with time for solar-mass models including gravity waves compared with observations in solar analogues. Updated from Meléndez *et al.* (2009).

being deposited in the radiative interior beyond the SLO. This is the filtered angular momentum luminosity  $\mathcal{L}_J^{\text{fil}}$ . Let us mention that in fact, the existence of a SLO is not even required to obtain this differential damping between prograde and retrograde waves, and thus, as long as differential rotation exists at the base of the convection zone, waves will have a net impact of the rotation rate of the interior.

The SLO's dynamics is studied by solving Eq. (2.4) with small time-steps and using the whole wave spectrum while for the secular evolution of the star, one has to use instead the filtered angular momentum luminosity. Let us stress that in the case of the secular evolution we do not follow the SLO dynamics, because of its very short time scale. Rather, we only consider the filtered angular momentum luminosity beyond the SLO, and its effect on chemicals is given by a local turbulence calculated from a study of the SLO's dynamic over very short time-scales. Let us also mention here that, for both the SLO and the filtered angular momentum luminosity, differential damping is required. Since this relies on the Doppler shift of the frequency (see Eqs. 2.2 and 2.3), angular momentum redistribution will be dominated by the low frequency waves that experience a larger Doppler shift, but that are not so low that they will be immediately damped. Numerical tests indicate that this occurs around  $\omega \simeq 1 \mu\text{Hz}$ .

### 3. The case of Population I low-mass stars, the Li dip and the Sun

An important property of IGWs is that their generation and efficiency in extracting angular momentum from stellar interiors depend on the structure of their convective envelope, which varies strongly with the effective temperature of the star. Figure 1 shows the  $T_{\text{eff}}$ -dependence of the filtered angular momentum luminosity of waves below the SLO, which directly measures the efficiency of wave-induced angular momentum extraction in zero-age main sequence stars around the Li dip. It appears that the net momentum luminosity slightly increases with increasing  $T_{\text{eff}}$ , presents a plateau, and suddenly drops

at the  $T_{\text{eff}}$  of the dip. This clearly indicates that the momentum transport by IGWs has the proper  $T_{\text{eff}}$ -dependence to be the required process to explain the cool side of the Li dip (Talon & Charbonnel 2003).

Talon *et al.* (2002) have shown, in a static model, that waves can efficiently extract angular momentum from a star that has a surface convection zone rotating slower than the interior. Charbonnel & Talon (2005) then calculated the evolution of the internal rotation profile for a solar-mass star with surface spin-down. We showed that, in that case, waves tend to slow down the core, creating “slow” fronts that propagate from the core to the surface (Fig. 2). These calculations confirmed, in a complete evolution of solar-mass models evolved from the pre-main sequence to 4.6 Gy, that IGWs play a major role in braking the solar core. This momentum transport reduces rotational mixing in low-mass stars, leading to a theoretical surface lithium abundance in agreement with observations made in solar analogues of various ages (Fig. 2).

Figure 1 shows our predictions for rotation velocities and Li surface abundances together with the observed data at the age of the Hyades. On the left side of the dip, IGWs play no role and the predictions are taken from Charbonnel & Talon (1999). On the cool side of the dip IGWs are at act and lead to the rise of the surface Li. The model at  $\sim 5800$  K corresponds to a  $1.0 M_{\odot}$  star. It was computed for 3 initial rotation velocities of 50, 80 and  $110 \text{ km s}^{-1}$  (Charbonnel & Talon 2005). Models with IGWs are in perfect agreement with the observations, both regarding the amplitude of the Li depletion and the dispersion at a given effective temperature.

#### 4. The case of Population II low-mass stars

In the context of primordial nucleosynthesis, it has long been debated whether Pop II stars could have depleted their surface Li abundance, just as their metal-rich counterpart did. Recent results on cosmic microwave background anisotropies, and especially those of the WMAP experiment, have firmly established that the primordial Li abundance is  $\sim 3$  to 5 times higher than the measured Li value in dwarf stars along the so-called Spite plateau (Charbonnel & Primas 2005). The main theoretical difficulty to reproduce these data is that the Li abundance is remarkably constant in halo dwarfs, while it seems at first sight that depletion should lead to a larger dispersion.

A re-examination of Li data in halo stars available in the literature has led to a very surprising result: the mean Li value as well as its dispersion appear to be lower for the dwarfs than for the subgiant stars (Charbonnel & Primas 2005). In addition, all deviant stars, i.e. those with a strong Li deficiency or an abnormally high Li content, lie on or originate from the hot side of the Li plateau. These results indicate that halo stars that have now just passed the turnoff have experienced a Li history slightly different from that of their less massive counterparts.

This behaviour is the signature of a transport process for angular momentum whose efficiency changes on the extreme blue edge of the plateau and it corresponds to the generation and filtering of IGWs in Pop II stars (Fig. 3, Talon & Charbonnel 2004), just as it does in the case of Pop I stars.

Indeed and as discussed previously, the generation of IGWs and, consequently, their efficiency in transporting angular momentum, depend on the structure of the stellar convective envelope, which in turn depends on the effective temperature of the star as can be seen in Fig. 3. As in the case of Pop I stars on the red side of the Li dip, the net angular luminosity of IGWs is very high and constant in Pop II stars along the plateau up to  $T_{\text{eff}} \sim 6300$  K. There, IGWs should dominate the transport of angular momentum and enforce quasi solid-body rotation of the stellar interior on very short timescale. As

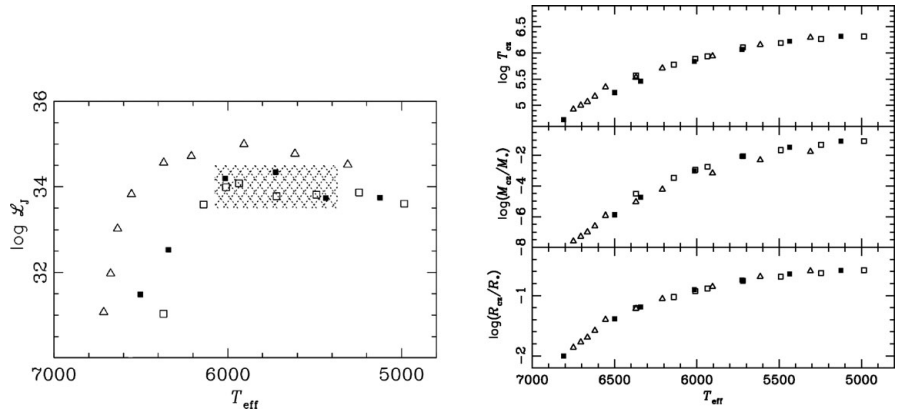


**Figure 3.** (Left) Net momentum luminosity at  $0.03 R_*$  below the surface convection zone as a function of  $T_{\text{eff}}$  for an initial differential rotation of  $\delta\Omega = 0.01 \mu\text{Hz}$  over  $0.05 R_*$ . The Li plateau region is dashed. From Charbonnel & Talon (2004). (Right) (top) Temperature at the base of the convection zone ( $T_{cz}$ ), (middle) mass of the convection zone and (bottom) radius of the convection zone as a function of  $T_{\text{eff}}$ . Squares: Pop II stars on the zams (open squares) and at 10 Gyr (black squares); Triangles: Pop I stars on the zams. From Charbonnel & Talon (2004).

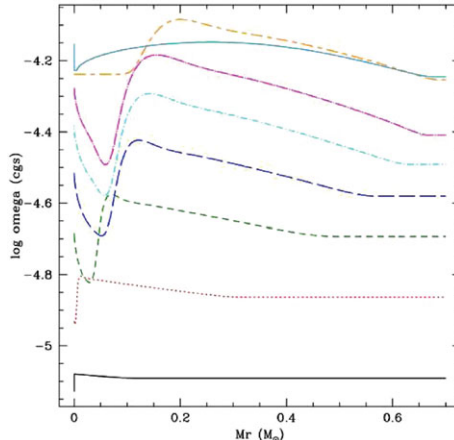


**Figure 4.** Evolution of the rotation profile inside a  $0.7 M_\odot$  Pop II star during the pre-main sequence. Curves correspond to 2, 5, 10, 15, 20, 25, 35 and 237 My, from bottom to top (acceleration is related to the star's overall contraction). The ZAMS velocity is  $25 \text{ km s}^{-1}$ .

a result, the surface Li depletion is expected to be independent of the initial angular momentum distribution, implying a very low dispersion of the Li abundance from star to star.

In more massive stars however the efficiency of IGWs decreases and internal differential rotation is expected to be maintained under the effect of meridional circulation and turbulence. Consistently, variations of the initial angular momentum from star to star would lead to more Li dispersion and to more frequent abnormalities in the case of the most massive stars where IGWs are not fully efficient, as required by the observations. We note that the mass-dependence of the IGWs efficiency also leads to a natural explanation of fast horizontal branch rotators.

*Let us stress here that the absence of a Li dip in Pop II stars reflects the facts that Pop II dip stars already evolved past the main sequence.*

We started the computation of complete stellar evolution models of Pop II stars from the pre-main sequence. Preliminary results show that the spin-down fronts that are observed in Pop I stars are also seen in Pop II stars during the PMS (see Fig. 4). Lithium depletion remains negligible during that phase. Calculation of the main sequence evolution is underway.

## 5. Conclusions

IGWs have a large impact on the evolution of low-mass stars, especially through their effect on the rotation profile, which then modifies meridional circulation and shear turbulence, and thus, the mixing of chemical elements. Within this framework, hydrodynamical models including the combined effects of meridional circulation, shear turbulence and internal gravity waves (using an excitation model that fits solar p-modes) successfully reproduce several observations:

- the time evolution of lithium in solar analogues (Fig. 2);
- the shape of the Li and Be dips (Fig. 1);
- the Li and Be behaviour in evolved stars (see Charbonnel & Lagarde, this Volume);
- the small amount of differential rotation measured by helioseismology (Fig. 2).

Up to now, no other theoretical model has achieved similar results. We also expect that IGWs can reduce the impact of the variety of initial rotation velocities during the spin-down phase of Pop II stars and thus, could be an important element in the understanding of the small amount of dispersion measured on the Li plateau.

Our comprehensive picture should have implications for other difficult unsolved problems related to the transport of chemicals and angular momentum in stars. We think in particular to the stars on the horizontal and asymptotic giant branches that exhibit unexplained abundance anomalies. No doubt that all these so-called “non-standard” physical processes must be part of the art of modelling stars in the 21<sup>st</sup> century. In this context, light elements such as Li and Be play a crucial role.

## Acknowledgements

We acknowledge financial support from IAU, from the French “Programme National de Physique Stellaire” of CNRS/INSU, and from the Swiss National Science Foundation.

## References

- Ando, H. 1986, *A&A*, 163, 97  
 Balachandran, S. 1995, *ApJ* 446, 203  
 Balmforth, N. J. 1992, *MNRAS* 255, 639  
 Boesgaard, A. M. & Tripicco, M. J. 1986, *ApJ*, 302, L49  
 Boesgaard, A. M. 1987, *PASP* 99, 1067  
 Brown, T. M., Christensen-Dalsgaard, J., Dziembowski, W. A., Goode, P., Gough, D. O., & Morrow, C. A. 1989, *ApJ* 343, 526  
 Burkhart, C. & Coupry, M. F. 2000, *A&A* 354, 216  
 Chaboyer, N., Demarque, P., Guenther, D. B., & Pinsonneault, M. H. 1995, *ApJ* 446, 435  
 Charbonneau, P. & Mac Gregor, K. B. 1993, *ApJ* 417, 762  
 Charbonnel, C. & Primas, F. 2005, *A&A* 442, 961  
 Charbonnel, C. & Talon, S. 1999, *A&A* 351, 635  
 Charbonnel, C. & Talon, S. 2005, *Science* 309, 2189  
 Charbonnel, C. & Talon, S. 2007, AIP Conference Proceedings, Volume 948, pp. 15-26  
 Couvidat, S., García, R. A., Turck-Chièze, S., Corbard, T., Henney, C. J., & Jiménez-Reyes, S. 2003, *ApJ* 597, L77  
 Deliyannis, C. P., King, J. R., & Boesgaard, A. M. 1997, Kontikas E., et al. (eds), “Wide-field spectroscopy”, p. 201

- Eggenberger, P., Maeder, A., & Meynet, G. 2005, *A&A*, 440, L9
- Fossati, L., Bagnulo, S., Landstreet, J., Wade, G., Kochukhov, O., Monier, R., Weiss, W., & Gebran, M. 2008, *A&A*, 483, 891
- Gaigé, Y. 1993, *A&A* 269, 267
- García, R. A., Turck-Chièze, S., Jiménez-Reyes, S. J., Ballot, J., Pallé, P. L., Eff-Darwich, A., Mathur, S., & Provost, J. 2007, *Science*, 316, 1591
- García López, R. J. & Spruit, H. C. 1991, *ApJ* 377, 268
- Gebran, M., Monier, R., & Richard, O. 2008, *A&A*, 479, 189
- Goldreich, P. & Kumar, P. 1990, *ApJ* 363, 694
- Goldreich, P., Murray, N., & Kumar, P. 1994, *ApJ* 424, 466
- Gough, D. O. & McIntyre, M. E. 1998, *Nature* 394, 755
- Kim, E. & MacGregor, K. B. 2001, *ApJ*, 556, L117
- Kiraga, M., Jahn, K., Stepien, K., & Zahn, J.-P. 2003, *Acta Astronomica* 53, 321
- Kosovichev, A., et al. 1997, *Sol. Phys.* 170, 43
- Kumar, P. & Quataert, E. J. 1997, *ApJ* 575, L143
- Kumar, P., Talon, S., Zahn, J.-P. 1999, *ApJ* 520, 859
- Maeder, A. 1995, *A&A*, 299, 84
- Maeder, A. & Meynet, G. 2000, *ARA&A* 38, 143
- Matias, J. & Zahn, J.-P. 1998, Provost & Schmider (eds), “*Sounding solar and stellar interiors*”, IAU Symp. 181
- Meléndez, J., Ramírez, I., Casagrande, L., Asplund, M., Gustafsson, B., Yong, D., Do Nascimento, J. D., Castro, M., & Bazot, M. 2009 *Ap&SS*, tmp, 221
- Michaud, G. 1986, *ApJ* 302, 650
- Montalban, J. 1994 *A&A*, 281, 421
- Montalban, J. & Schatzman E. 1996 *A&A*, 305, 513
- Montalban, J. & Schatzman E. 2000 *A&A*, 354, 943
- Palacios, A., Talon, S., Charbonnel, C., & Forestini, M. 2003, *A&A* 399, 603
- Pasquini, L., Randich, S., Zoccali, M., Hill, V., Charbonnel, C., & Nordström, B. 2004, *A&A* 424, 951
- Pilachowski, C. A., Saha, A., & Hobbs, L. M. 1988, *PASP* 100, 474
- Pinsonneault, M. H., Kawaler, S. D., Sofia, S., & Demarque, P. 1989 *ApJ* 338, 424
- Press, W. H. 1981 *ApJ*, 245, 286
- Ringot, O. 1998, *A&A* 335, 89
- Rogers, T. M. & Glatzmaier, G. A. 2005a, *ApJ*, 620, 432
- Rogers, T. M. & Glatzmaier, G. A. 2005b, *MNRAS*, 364, 1135
- Schatzman, E. 1993 *A&A* 279, 431
- Smiljanic, R., Pasquini, L., Charbonnel, C., & Lagarde, N., 2009 arXiv0910.4399, *A&A*, in press
- Takeda, Y., Kawanomoto, S., Takada-Hidai, M., & Sadakane, K. 1998, *PASJ* 50, 509
- Talon S. 1997 *PhD Thesis*, Université Paris VII
- Talon, S., Kumar, P., Zahn, J.-P. 2002, *ApJL* 574, 175
- Talon, S. & Charbonnel, C. 1998, *A&A* 335, 959
- Talon, S. & Charbonnel, C. 2003, *A&A* 405, 1025
- Talon, S. & Charbonnel, C. 2004, *A&A* 418, 1051
- Talon, S. & Charbonnel, C. 2005, *A&A* 440, 981
- Talon, S., Richard, O., & Michaud, G. 2006, *ApJ* 645, 634
- Talon, S. & Zahn, J. P. 1998, *A&A*, 329, 315
- Théado, S. & Vauclair, S. 2003, *ApJ*, 587, 795
- Townsend A. A., 1958, *J. Fluid Mech.* 4, 361
- Varenne, O. & Monier R. 1999 *A&A* 351, 247
- Wallerstein, G., Herbig G. H., & Conti, P. S. 1965, *ApJ*, 141, 610
- Young, P. A., Knierman, K. A., Rigby, J. R., & Arnett, D. 2003, *ApJ*, 585, 1114
- Zahn, J. P. 1992, *A&A* 265, 115
- Zahn, J. P., Talon, S., & Matias, J. 1997, *A&A* 322, 320